Bending examination of advanced generation of composite structures with specific properties exposed to different loads

Ahmed Zitouni[a], *Bachir* Bouderba[b], *Abdelkader* Dellal[c], *Hamza Madjid* Berrabah[d]

[a] Tissemsilt University, Department of Science and Technology, Mechanical Engineering Materials and Structures Laboratory, Tissemsilt, People's Democratic Republic of Algeria, e-mail: ahmed.zitouni@univ-tissemsilt.dz,**corresponding author**, ORCID iD: https://orcid.org/0000-0003-1627-6020

[b] Tissemsilt University, Department of Science and Technology, Mechanical Engineering Materials and Structures Laboratory, Tissemsilt, People's Democratic Republic of Algeria, e-mail: bouderba.bachir@univ-tissemsilt.dz, ORCID iD: https://orcid.org/0000-0003-4668-122X

[c] Tissemsilt University, Department of Science and Technology, Tissemsilt, People's Democratic Republic of Algeria, e-mail: dellal.abdelkader@univ-tissemsilt.dz, ORCID iD: https://orcid.org/0009-0003-2305-4845

[d] University of Relizane, Department of Civil Engineering, Mechanical Engineering Materials and Structures Laboratory, Relizane, People's Democratic Republic of Algeria, e-mail: b_hamza_2005@yahoo.fr, ORCID iD: https://orcid.org/0000-0002-7871-4017

DOI: https://doi.org/10.5937/vojtehg72-47852

FIELD: mechanics
ARTICLE TYPE: original scientific paper

Abstract:

Introduction/purpose: This article presents the bending examination of advanced-generation composite structures with specific properties exposed to different loads.

Methods: This paper thus proposes and introduces a new generalized five-variable shear strain theory for calculating the static response of functionally graded rectangular plates made of ceramic and metal. Notably, our theory eliminates the need for a shear correction factor and ensures zero-shear stress conditions on both the upper and lower surfaces. Numerical investigations are introduced to interpret the influences of loading conditions and variations of power of functionally graded material, modulus ratio, aspect ratio, and thickness ratio on the bending behavior of FGPs. These analyzes are then compared to the results available in the literature.

Results: Preliminary results include a comparative analysis with standard higher-order shear deformation theories (PSDPT, ESDPT, SSDPT), as well as Mindlin and Kirchhoff theories (FSDPT and CPT).

Conclusion: Our theory contributes alongside established theories in the field, providing valuable insights into the static thermomechanical response of functionally graded rectangular plates. This encompasses the influence of volume fraction exponent values on nondimensional displacements and stresses, the impact of aspect ratios on deflection, and the effects of the thermal field on deflection and stresses. Numerical examples of the bending examination of advanced-generation composite structures with specific properties exposed to different loads demonstrate the accuracy of the present theory.

Key words: functionally graded materials, bending, higher-order shear deformation theories, thermomechanical.

Introduction

Composites are materials formed by combining two or more constituent materials to create superior properties, defying traditional material constraints.

They are commonly used in aerospace, automotive, construction, and many other industries due to their exceptional strength-to-weight ratio (where the quest for ever-lighter and stronger materials is a perpetual challenge) as well as good performance.

Despite these good properties, however, there is a negative aspect that worries industrialists and researchers; it is the failure in difficult operational environments. It shows signs of failure and disintegration.

Composite materials, while versatile, can deteriorate over time due to weakening interfaces between their layers (Pindera et al, 1998; Boggarapu et al, 2021), leading to performance issues and failures. In response to these challenges, functionally graded materials (FGMs) have emerged as a progressive development in material science.

Functionally graded materials (FGMs) indeed represent an innovative and sophisticated approach to addressing some of the challenges associated with conventional composite materials. FGMs are designed to provide tailored material properties by gradually changing, or grading, the composition, structure, and properties of the material in a specific direction. This gradient-based approach offers several advantages for various engineering and industrial applications.

In 1984, a group of researchers in Sendai, Japan (Koizumi, 1993; Koizumi & Niino, 1995; Koizumi, 1997), introduced the concept of Functionally Graded Materials (FGMs). These materials are characterized

by their uninterrupted variation in properties, distinguishing them from conventional materials.

Functionally graded materials (FGMs) find application across diverse industries (Kieback et al, 2003), and recent research illuminates their behavior under thermal and mechanical loads. Classical plate theories, like CPT, lack accuracy for thicker structures (Bouazza et al, 2011). The First-Order Shear Deformation Theory (FSDT) (Reissner, 1945; Mindlin, 1951; Timoshenko & Woinowsky-Krieger, 1959) addressed this but needs a corrective factor. Higher-order shear deformation theories (HSDT) excel, showing improved accuracy without requiring a correction factor, unlike previous models.

In this context, Reddy (2000) studied the static behavior of FGM plates using the third-order shear deformation theory. Zenkour & Alghamdi (2010) explored the bending behavior of sandwich plates, investigating the impacts of thermomechanical loads on stresses and deflections. Additionally, Bouderba & Benyamina (2018) introduced a model for analyzing the thermal-mechanical behavior of thick metal/ceramic FGM plates.

Li et al. (2020) introduced a new five-variable shear deformation theory for predicting the static response of functionally graded plates. Daikh et al. (2020) studied the thermomechanical bending behavior of functionally graded sandwich plates under varied temperatures. Brischetto & Carrera (2010) proposed enhanced mixed theories, while Benyamina et al (2018) examined composite material plates in thermal settings, contributing to a deeper understanding of their performance.

Bouderba et al. (2016) used a simple shear deformation theory to examine the thermal stability of FGM sandwich plates. Shinde et al. (2015) introduced a refined trigonometric shear deformation theory for the analysis of bending in both isotropic and orthotropic plates under a variety of loading conditions. In a related vein, Bouderba & Berrabah (2022) delved into the bending response of porous advanced composite functionally graded material (FGM) plates subjected to thermomechanical loads.

Zenkour & Hafed (2020) conducted a study on the bending analysis of functionally graded piezoelectric (FGP) material plates under simply supported edge conditions. They employed a simple quasi-3D sinusoidal shear deformation theory for their analysis. In another study, Brischetto et al (2008) examined the deformations of a simply supported rectangular plate composed of functionally graded material (FG) subjected to both thermal and mechanical loads.

On the other hand, Berrabah & Bouderba (2023) employed an accurate shear deformation theory to investigate the mechanical buckling behavior of FG plates. Furthermore, higher-order plate theories have been introduced in the literature to address the mechanical and thermal buckling of FG plates, with the Carrera unified formulation being utilized (Farrokh et al, 2021; Farrokh et al, 2022).

This paper aims to comprehensively examine advanced composite structures under varied loads, focusing specifically on a rectangular plate made of functionally graded material (FGM) subjected to mechanical and thermal stress. Using the novel CSDPT theory with five unknown variables, the study derives and solves the equations of motion through Navier's procedure. Validation occurs through comparative analyses with standard higher-order theories like PSDPT, SSDPT, and ESDPT. The study's outcomes illuminate the impact of the power index on non-dimensional displacement and stresses, addressing the thermal field's influence on deflection and stresses in the FGM plate. This examination significantly contributes to understanding the behavior of these structures under different load conditions, advancing the field of mechanical construction.

Essential formulation

Structure geometry and material gradient

Geometry of the structure of the FGM (in the context of the plate)

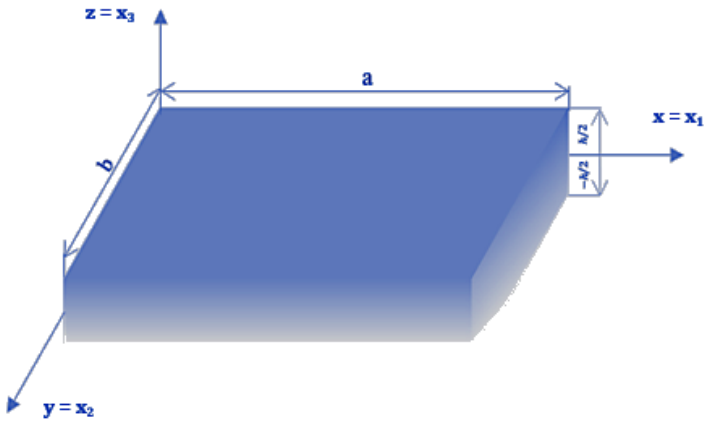

Figure 1 – Geometry and the coordinate system of the FGM

In the context of our research on advanced composite structures, the geometric characteristics of the rectangular plate made of functionally graded material (FGM) play a pivotal role. This plate, as depicted in Figure1, exhibits specific material properties that transition gradually from the bottom to the top surface.

Table 1 – Geometric properties of the functionally graded plate.

Characte-ristics	Structure geometry	Thickness	Length	Width	Aspect ratio	Material coordinate origin (x_3)
Symbol	-	h	a	B	a/b	x_3
Description	Rectangular plate	Plate thickness (x_3-axis)	Plate length (x_1-axis)	Plate width (x_2-axis)	Aspect ratio of the plate	Middle of the plate thickness ($x_3 = \pm h / 2$)

Material gradient in the FGM plate

In the context of functionally graded material (FGM) plates, material attributes, including Young modulus (E), Poisson's ratio (v), and thermal dilation coefficient (α), are defined by applying the mixing rule (1) (Reddy, 2000) and utilizing the Power-Law function (2).

$$P(x_3) = (P_c - P_m)V\left(x_3\right) + P_m \quad (1)$$

$$V\left(x_3\right)=(1/2+x_3/h)^n \quad (2)$$

Material properties can be described by the following equation:

$$E(x_3) = (E_c - E_m)(1/2 + x_3 / h)^n + E_m \quad (3)$$

The gradient law for Young's modulus (E) (3), applies to Poisson's ratio (v) and the coefficient of thermal expansion (α) as well.

Here, x_3 signifies the position along the plate's thickness, h is the total thickness, and n is a material parameter influencing the composition gradation.

The material properties (E_m, ν_m, α_m) and (E_c, ν_c, α_c) are associated with the metallic and ceramic phases, respectively.

Table 2 – Transverse shear strain functions for the FGM plate.

Theories, the author	**Form of function f(z)**
Parabolic deformation theory of plates, (Reissner, 1945)	$5z/4(1-(4/3)(z/h)^2)$
Parabolic shear deformation theory (PSDPT), (Reddy, 1984)	$z(1-(4/3)(z/h)^2)$
Trigonometric deformation theory of plates (SSDPT), (Touratier, 1991)	$(h/\pi)\sin(\pi z/h)$
The exponential shear deformation plate theory (ESDPT), (Karama et al, 2003)	$ze^{-2(z/h)^2}$
Hyperbolic deformation theory of plates, (Soldatos, 1992)	$z\cosh(1/2)-h\sinh(z/h)$
Combination functions(CSDPT), Present	$\frac{(e^2+1)\arctan(e^{2z/h})}{(e-1)^2}-\frac{2ez}{h(e-1)^2}-\frac{\pi(e^2+1)}{4(e-1)^2}$

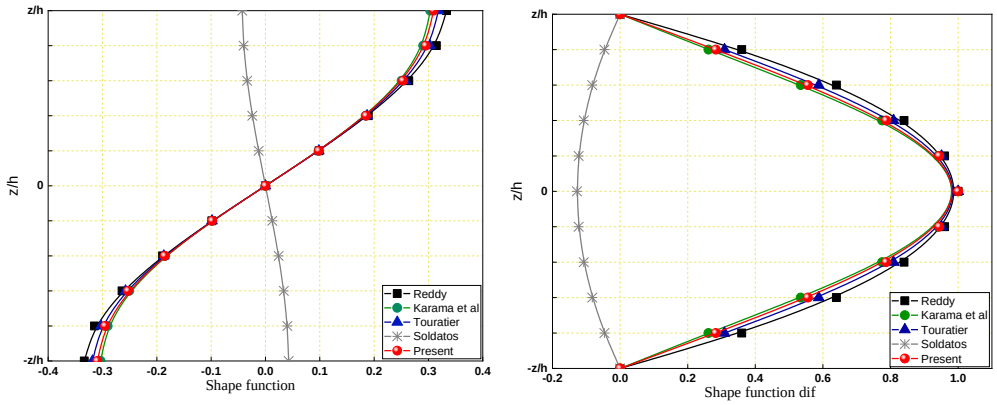

Figure 2 – Distribution of the functions f (z):
(a)shape function f(z),
(b) differentiation f´(z)

Figure 2 provides a comparison of how the shape function and its derivatives vary across different shear deformation theories, denoted as f(z) and its derivative f'(z).

Table 3 – Material properties - metal and ceramic materials, see (Bao & Wang, 1995; Bouderba & Berrabah, 2022)

Property	Young's modulus		Poisson's ratio		Thermal expansion coefficient		Density	
Symbol	E_{metal}	$E_{ceramic}$	ν_{metal}	$\nu_{ceramic}$	α_{metal}	$\alpha_{ceramic}$	ρ_{metal}	$\rho_{ceramic}$
Value	70	151	0.3	0.3	23	10	7.8	7.8
Descrip-tion	Elastic modulus of the material in GPa		Poisson's ratio of the material		Linear coefficient of thermal expansion ($x10^{-6}$/°C)		Density of the material in g/cm³	

Theoretical formulation

Formulating the displacement field

In the context of thick functionally graded material (FGM) plates, the displacement of a material point at the coordinates (x_1, x_2, x_3) could be expressed as follows:

$$U(x_1,x_2,x_3)=u_0(x_1,x_2)-x_3\frac{\partial w_0}{\partial x_1}+\Phi(x_3)\Theta_{x_1}$$

$$V(x_1,x_2,x_3)=v_0(x_1,x_2)-x_3\frac{\partial w_0}{\partial x_2}-\Phi(x_3)\Theta_{x_2} \quad (4)$$

$$W(x_1,x_2,x_3)=w_0(x_1,x_2)$$

The mid surface of the structure is characterized by five unknown displacement functions, namely u_0, v_0, w_0, and $\Theta_{x_1}, \Theta_{x_2}$.

Based on the equations describing the displacement within the field and the relationships governing strain-displacement, we deduce expressions for the strain elements derived from the displacement elements.

$$\begin{Bmatrix}\varepsilon_{11}\\ \varepsilon_{22}\\ \gamma_{12}\end{Bmatrix}=\begin{Bmatrix}\dfrac{\partial u_0}{\partial x_1}-x_3\dfrac{\partial^2 w_0}{\partial {x_1}^2}+\Phi(x_3)\dfrac{\partial\Theta_{x_1}}{\partial x_1}\\ \dfrac{\partial v_0}{\partial x_2}-x_3\dfrac{\partial^2 w_0}{\partial {x_2}^2}+\Phi(x_3)\dfrac{\partial\Theta_{x_2}}{\partial x_2}\\ \left(\dfrac{\partial v_0}{\partial x_1}+\dfrac{\partial u_0}{\partial x_2}\right)-x_3\dfrac{2\partial^2 w_0}{\partial x_1\partial x_2}+\Phi(x_3)\left(\dfrac{\partial\Theta_{x_2}}{\partial x_1}+\dfrac{\partial\Theta_{x_1}}{\partial x_2}\right)\end{Bmatrix} \quad (5a)$$

$$\gamma_{23} = \frac{d\Phi(x_3)}{dx_3}.\Theta_{x_2}, \gamma_{13} = \frac{d\Phi(x_3)}{dx_3}.\Theta_{x_1} \qquad \text{(5b, 5b')}$$

where $\varepsilon_{11}, \varepsilon_{22}, \gamma_{12}, \gamma_{23}$ and γ_{13} are the strain and shear components, respectively.

Equations (5a) and (5b, 5b') can be expressed like this:

$$\begin{Bmatrix} \varepsilon_{11} \\ \varepsilon_{22} \\ \gamma_{12} \end{Bmatrix} = \begin{Bmatrix} \varepsilon_{11}^0 \\ \varepsilon_{22}^0 \\ \gamma_{12}^0 \end{Bmatrix} + x_3 \begin{Bmatrix} k_{11}^0 \\ k_{22}^0 \\ k_{12}^0 \end{Bmatrix} + \Phi(z) \begin{Bmatrix} k_{11}^1 \\ k_{22}^1 \\ k_{12}^1 \end{Bmatrix}, \qquad (6)$$

$$\gamma_{23} = \Phi'(x_3).\gamma_{23}^0, \gamma_{13} = \Phi'(x_3).\gamma_{13}^0, \gamma_{33} = 0.$$

The stress-strain relationships can be concisely expressed with the following equation:

$$\begin{Bmatrix} \sigma_{11} \\ \sigma_{22} \\ \sigma_{33} \\ \tau_{12} \\ \tau_{23} \\ \tau_{13} \end{Bmatrix} = \begin{bmatrix} Q_{11} & Q_{12} & Q_{13} & 0 & 0 & 0 \\ Q_{12} & Q_{22} & Q_{23} & 0 & 0 & 0 \\ Q_{13} & Q_{23} & Q_{33} & 0 & 0 & 0 \\ & & & Q_{66} & 0 & 0 \\ & & & & Q_{44} & 0 \\ Sym & & & & & Q_{55} \end{bmatrix} \begin{Bmatrix} \varepsilon_{11} \\ \varepsilon_{22} \\ \varepsilon_{33} \\ \gamma_{12} \\ \gamma_{23} \\ \gamma_{13} \end{Bmatrix} \qquad (7)$$

The following equation considers the influence of thermal effects:

$$\begin{Bmatrix} \sigma_{11} \\ \sigma_{22} \\ \tau_{12} \end{Bmatrix} = \begin{bmatrix} Q_{11} & Q_{12} & 0 \\ & Q_{22} & 0 \\ Sym & & Q_{66} \end{bmatrix} \left(\begin{Bmatrix} \varepsilon_{11} \\ \varepsilon_{12} \\ \gamma_{12} \end{Bmatrix} - \begin{Bmatrix} \alpha(x_3)\,\Delta T \\ \alpha(x_3)\,\Delta T \\ 0 \end{Bmatrix} \right) \qquad \text{(8a)}$$

$$\begin{Bmatrix} \tau_{23} \\ \tau_{13} \end{Bmatrix} = \begin{bmatrix} Q_{44} & 0 \\ Sym & Q_{55} \end{bmatrix} \begin{Bmatrix} \gamma_{23} \\ \gamma_{13} \end{Bmatrix} \qquad \text{(8b)}$$

The parameters $(\sigma_{11}, \sigma_{22}, \tau_{12}, \tau_{23}, \tau_{13})$ and $(\varepsilon_{11}, \varepsilon_{22}, \gamma_{12}, \gamma_{23}, \gamma_{13})$ represent the stress and deformation components, respectively.

The mathematical formulation of the stiffness coefficients Q_{ij} is as follows:

$$Q_{11} = Q_{22} = Q_{33} = \frac{E(x_3)}{1-\nu^2}, \quad Q_{12} = \frac{\nu\, E(x_3)}{1-\nu^2}, Q_{44} = Q_{55} = Q_{66} = \frac{E(x_3)}{2(1+\nu)} \qquad \text{(9a, 9b, 9c)}$$

The temperature distribution $T(x_1, x_2, x_3)$ through thickness is assumed as Bouderba et al. (2013).

The following equation describes how temperature varies through the thickness of the plate:

$$T(x_1, x_2, x_3) = T_1(x_1, x_2) + \frac{x_3}{h} T_2(x_1, x_2) + \bar{\Phi}(x_3) T_3(x_1, x_2) \qquad (10)$$

In this study, we focused on employing the sinusoidal temperature distribution to conduct our analysis $\bar{\Phi}(x_3) = \frac{1}{\pi}\sin(x_3 \frac{\pi}{h})$.

Governing equations

Formulating the equilibrium governing equations involves applying the principle of virtual work, which can be articulated in the following manner in this context:

$$\begin{aligned}
&\partial N_{11}/\partial x_1 + \partial N_{12}/\partial x_2 = 0 \\
&\partial N_{22}/\partial x_2 + \partial N_{12}/\partial x_1 = 0 \\
&\partial^2 M_{11}/\partial {x_1}^2 + 2\partial^2 M_{12}/\partial x_1 \partial x_2 + \partial^2 M_{22}/\partial {x_2}^2 + q = 0 \qquad (11) \\
&\partial S_{11}/\partial x_1 + \partial S_{12}/\partial x_2 - Q_{13} = 0 \\
&\partial S_{22}/\partial x_2 + \partial S_{12}/\partial x_1 - Q_{23} = 0
\end{aligned}$$

N, M, and S are the quantities that represent the force and moment resultants, and their definitions are as follows:

$$\begin{Bmatrix} N_{11} & N_{22} & N_{12} \\ M_{11} & M_{22} & M_{12} \\ S_{11} & S_{22} & S_{12} \end{Bmatrix} = \int_{h_1}^{h_2} (\sigma_{11}, \sigma_{22}, \sigma_{12}) \begin{Bmatrix} 1 \\ x_3 \\ \Phi(x_3) \end{Bmatrix} dx_3, \qquad \text{(12a)}$$

$$(Q_{13}, Q_{23}) = \int_{h_1}^{h_2} (\tau_{13}, \tau_{23}) \Phi'(x_3) dx_3, \qquad \text{(12b)}$$

The interval limits for simplification: $-h/2 = h_1$, $h/2 = h_2$,

$$\begin{Bmatrix} N \\ M \\ S \end{Bmatrix} = \begin{bmatrix} A & B & B^a \\ & D & D^a \\ Sym & & F^a \end{bmatrix} \begin{Bmatrix} \varepsilon^0 \\ k^0 \\ k^1 \end{Bmatrix} - \begin{Bmatrix} N^T \\ M^T \\ S^T \end{Bmatrix}, \tag{13a}$$

$$Q_{23} = A_{44}^a \gamma_{23}, Q_{13} = A_{55}^a \gamma_{13}. \tag{13b}$$

$$N = \{N_{11}, N_{22}, N_{12}\}^t, M = \{M_{11}, M_{22}, M_{12}\}^t, S = \{S_{11}, S_{22}, S_{12}\}^t,$$

$$N^T = \{N_{11}^T, N_{22}^T, 0\}^t, M^T = \{M_{11}^T, M_{22}^T, 0\}^t, S^T = \{S_{11}^T, S_{22}^T, 0\}^t, \tag{13c}$$

$$\varepsilon^0 = \{\varepsilon_{11}^0, \varepsilon_{22}^0, \gamma_{12}^0\}^t, k^0 = \{k_{11}^0, k_{22}^0, k_{12}^0\}^t, k^1 = \{k_{11}^1, k_{22}^1, k_{12}^1\}^t,$$

The following can be deduced:

$$A = \begin{bmatrix} A_{11} & A_{12} & 0 \\ & A_{22} & 0 \\ Sym & & A_{66} \end{bmatrix}, B = \begin{bmatrix} B_{11} & B_{12} & 0 \\ & B_{22} & 0 \\ Sym & & B_{66} \end{bmatrix}, B^a = \begin{bmatrix} B_{11}^a & B_{11}^a & 0 \\ & B_{11}^a & 0 \\ Sym & & B_{66}^a \end{bmatrix},$$

$$D = \begin{bmatrix} D_{11} & D_{12} & 0 \\ & D_{22} & 0 \\ Sym & & D_{66} \end{bmatrix}, D^a = \begin{bmatrix} D_{11}^a & D_{12}^a & 0 \\ & D_{22}^a & 0 \\ Sym & & D_{66}^a \end{bmatrix}, F^a = \begin{bmatrix} F_{11}^a & F_{12}^a & 0 \\ & F_{22}^a & 0 \\ Sym & & F_{66}^a \end{bmatrix} \tag{14a}$$

$$Q = \{Q_{23}, Q_{13}\}^t, \gamma = \{A_{23}^0, A_{13}^0\}^t, A^a = \begin{bmatrix} A_{44}^a & 0 \\ 0 & A_{55}^a \end{bmatrix} \tag{14b}$$

The stiffness coefficients, denoted as A_{ij}, B_{ij}, are defined as follows:

(15a)

$$\begin{Bmatrix} A_{11} & B_{11} & D_{11} & B_{11}^a & D_{11}^a & F_{11}^a \\ A_{12} & B_{12} & D_{12} & B_{12}^a & D_{12}^a & F_{12}^a \\ A_{66} & B_{66} & D_{66} & B_{66}^a & D_{66}^a & F_{66}^a \end{Bmatrix} = \int_{h_1}^{h_2} Q_{11} \left(1, x_3, x_3^2, \Phi(x_3), x_3\ \Phi(x_3), \Phi^2(x_3)\right) \begin{Bmatrix} 1 \\ \nu \\ \frac{1-\nu}{2} \end{Bmatrix} dx_3,$$

$$\left(A_{22}, B_{22}, D_{22}, B_{22}^a, D_{22}^a, F_{22}^a\right) = \left(A_{11}, B_{11}, D_{11}, B_{11}^a, D_{11}^a, F_{11}^a\right),$$

$$A_{ii}^a = \int_{h_1}^{h_2} \frac{E(x_3)}{2(1+\nu)} \left[\Phi'(x_3)\right]^2 dx_3, (i = 4, 5) \tag{15b}$$

The stress and moment resultants on a plate element $N_{11}^T = N_{22}^T, M_{11}^T = M_{22}^T, S_{11}^T = S_{22}^T$, due to thermal loads are defined respectively by:

$$\begin{Bmatrix} N_{ii}^T \\ M_{ii}^T \\ S_{ii}^T \end{Bmatrix} = \int_{h_1}^{h_2} \frac{E(x_3)}{(1-\nu)} \alpha(x_3) T \begin{Bmatrix} 1 \\ x_3 \\ \Phi(x_3) \end{Bmatrix} dx_3, (i=1) \tag{16}$$

Substituting Eq. (13a, 13b) into Eq. (11), we obtain the following equations:

$$(A_{66}d_{22} + A_{11}d_{11})u_0 + (A_{66} + A_{12})d_{12}v_0 - (2B_{66} + B_{12})d_{122}w_0$$
$$-B_{11}d_{111}w_0 + (B_{66}^a d_{22} + B_{11}^a d_{11})\Theta_{x_1} + (B_{66}^a + B_{12}^a)d_{12}\Theta_{x_2} = p_1, \tag{17a}$$

$$(A_{66} + A_{12})d_{12}u_0 + (A_{22}d_{22} + A_{66}d_{11})v_0 - (2B_{66} + B_{12})d_{112}w_0$$
$$-B_{22}d_{222}w_0 + (B_{66}^a + B_{12}^a)d_{12}\Theta_{x_1} + (B_{22}^a d_{22} + B_{66}^a d_{11})\Theta_{x_2} = p_2, \tag{17b}$$

$$-(B_{12} + 2B_{66})d_{122}u_0 - B_{11}d_{111}u_0 - (B_{12} + 2B_{66})d_{112}v_0 - B_{22}d_{222}v_0$$
$$+(D_{11}d_{1111} + D_{22}d_{2222})w_0 + 2(D_{12} + 2D_{66})d_{1122}w_0 - (D_{12}^a + 2D_{66}^a)d_{122}\Theta_{x_1}$$
$$-D_{11}^a d_{111}\Theta_{x_1} - (D_{12}^a + 2D_{66}^a)d_{112}\Theta_{x_2} - D_{22}^a d_{222}\Theta_{x_2} = p3, \tag{17c}$$

$$(B_{66}^a d_{22} + B_{11}^a d_{11})u_0 + (B_{66}^a + B_{12}^a)d_{12}v_0 - D_{11}^a d_{111}w_0$$
$$-(D_{12}^a + 2D_{66}^a)d_{122}w_0 + (F_{11}^a d_{11} + F_{66}^a d_{22} - A_{44}^a)\Theta_{x_1} + (F_{12}^a + F_{66}^a)d_{12}\Theta_{x_2} = p4, \tag{17d}$$

$$(B_{66}^a + B_{12}^a)d_{12}u_0 + (B_{66}^a d_{11} + B_{22}^a d_{22})v_0 - D_{22}^a d_{222}w_0$$
$$-(D_{12}^a + 2D_{66}^a)d_{112}w_0 - (F_{12}^a + F_{66}^a)d_{12}\Theta_{x_1} + (F_{22}^a d_{22} + F_{66}^a d_{11} - A_{55}^a)d_{12}\Theta_{x_2} = p5, \tag{17e}$$

In this context, $\{p\} = \{p_1, p_2, p_3, p_4, p_5\}^t$ is a force vector, d_{ij}, d_{ijl} and d_{ijlm} are the following differential operators:

$$d_{ij} = \frac{\partial^2}{\partial x_{1_i} \partial x_{1_j}}, d_{ijl} = \frac{\partial^3}{\partial x_{1_i} \partial x_{1_j} \partial x_{1_l}}, d_{ijlm} = \frac{\partial^4}{\partial x_{1_i} \partial x_{1_j} \partial x_{1_l} \partial x_{1_m}}, \tag{18}$$
$$d_i = \frac{\partial}{\partial x_{1_i}}, (i, j, l, m = 1, 2), (x_{1_i} = x_1; x_{1_j} = x_2),$$

The components of the generalized force vector $\{p\}$ are defined as follows:

$$p_1 = \frac{\partial N_{11}^T}{\partial x_1}, p_2 = \frac{\partial N_{22}^T}{\partial x_2}, p_3 = q - \frac{\partial^2 M_{11}^T}{\partial x_1^2} - \frac{\partial^2 M_{22}^T}{\partial x_2^2}, p_4 = q - \frac{\partial^2 S_{11}^T}{\partial x_1^2} - \frac{\partial^2 S_{22}^T}{\partial x_2^2}, \tag{19}$$

Determining exact solutions for functionally graded plate structures

Rectangular plates are typically categorized based on the nature of their support systems. In this context, we are concerned with the specific boundary conditions associated with a simple support configuration.

$$\begin{aligned} v_0 &= w_0 = \Theta_{x_2} = N_{11} = M_{11} = S_{11} = 0 \ \ at\, x_1 = 0, a, \\ u_0 &= w_0 = \Theta_{x_1} = N_{22} = M_{22} = S_{22} = 0 \ \ at\, x_2 = 0, b, \end{aligned} \tag{20}$$

The displacement functions q_i and T_i can be expanded in the following manner, aligning them with both the boundary conditions and the governing equations. This expansion is characterized by the use of a double Fourier series.

$$\begin{Bmatrix} q \\ T_k \end{Bmatrix} = \begin{Bmatrix} q_0 \\ t_k \end{Bmatrix} \sin(i\, x_1)\sin(j\, x_2), (k = 1,\ 2,\ 3) \tag{21}$$

where $i = \pi / a$, $j = \pi / b$, q_0 and t_k are constants.

Following the procedure of the Navier solution, we assume the following solution:

$$\begin{Bmatrix} u_0 \\ v_0 \\ w_0 \\ \Theta_{x_1} \\ \Theta_{x_2} \end{Bmatrix} = \begin{Bmatrix} U\cos(i\, x_1)\sin(j\, x_2) \\ V\sin(i\, x_1)\cos(j\, x_2) \\ W\sin(i\, x_1)\sin(j\, x_2) \\ X\cos(i\, x_1)\sin(j\, x_2) \\ Y\sin(i\, x_1)\cos(j\, x_2) \end{Bmatrix}, \tag{22}$$

where the arbitrary parameters U, V, W, X and Y are used to determine the conditions in which the solution of equation (22) satisfies equilibrium equations (17). The following operator's equation is obtained:

$$\{\Delta\}[\Omega] = \{P\}, \tag{23}$$

$\{\Delta\}=\{U,V,W,X,Y\}^t$ and $[\Omega]$ is the symmetrical matrix, in which:

$$\begin{aligned}
&\Omega_{11}=-\left(A_{11}i^2+A_{66}j^2\right),\Omega_{12}=-i\,j\,\left(A_{12}+A_{66}\right),\Omega_{13}=i\,[B_{11}i^2+(B_{12}+2B_{66})\,j^2],\\
&\Omega_{14}=-\left(B^a_{11}i^2+B^a_{66}j^2\right),\Omega_{15}=-i\,j\,\left(B^a_{12}+B^a_{66}\right),\Omega_{22}=-\left(A_{66}i^2+A_{22}j^2\right),\\
&\Omega_{23}=j\,[B_{12}i^2+2B_{66}i^2+B_{22}j^2],\Omega_{24}=-i\,j\,\left(B^a_{12}+B^a_{66}\right),\Omega_{25}=-\left(B^a_{66}i^2+B^a_{22}j^2\right),\\
&\Omega_{33}=-\,[D_{11}i^4+2D_{12}i^2j^2+4D_{66}i^2j^2+D_{22}j^4],\\
&\Omega_{34}=i\,[D^a_{11}i^2+D^a_{12}j^2+2D^a_{66}j^2],\Omega_{35}=j\,[D^a_{12}i^2+2D^a_{66}i^2+E_{22}j^2],\\
&\Omega_{44}=-\,[F^a_{11}i^2+F^a_{66}j^2+A^a_{44}],\Omega_{45}=-i\,j\,\left(F^a_{12}+F^a_{66}\right),\Omega_{55}=-\,[F^a_{66}i^2+F^a_{22}j^2+A^a_{55}],
\end{aligned}\tag{24}$$

The components of the generalized forces vector are given by:

$$\begin{aligned}
&P_1=i\left(A^Tt_1+B^Tt_2+B^T_at_3\right),P_2=j\left(A^Tt_1+B^Tt_2+B^T_at_3\right),\\
&P_3=-q_0-h\left(i^2+j^2\right)\left(B^Tt_1+D^Tt_2+D^T_at_3\right),\\
&P_4=ih\left(B^T_at_1+D^T_at_2+F^T_at_3\right),P_5=jh\left(B^T_at+D^T_at_2+F^T_at_3\right),
\end{aligned}\tag{25}$$

$$\left\{A^T,B^T,D^T\right\}=\int_{h_1}^{h_2}\frac{E(x_3)}{1-\nu}\alpha(x_3)\left\{1,\bar{x}_3,\bar{x}_3^2\right\}dx_3,\tag{26}$$

$$\left\{B^T_a,D^T_a,F^T_a\right\}=\int_{h_1}^{h_2}\frac{E(x_3)}{1-\nu}\alpha(x_3)\bar{\Phi}(x_3)\left\{1,\bar{x}_3,\bar{\Phi}(x_3)\right\}dx_3,\tag{27}$$

It is important to note $\bar{x}_3=x_3/h,\bar{\Phi}(x_3)=\Phi(x_3)/h$.

Analytical validation and numerical results

This section examines how materials respond to bending under thermal and mechanical loads. It aims to verify the accuracy of the theory and explore the effects of the parameters on bending, using the following non-dimensional parameters in the calculations:

The central deflection $\bar{w}=\frac{10^2D}{a^4q_0}w\left(\frac{a}{2},\frac{b}{2}\right)$, axial stress $\bar{\sigma}_{11}=\frac{1}{10^2q_0}\sigma_{11}\left(\frac{a}{2},\frac{b}{2},\frac{h}{2}\right)$,

The longitudinal shear stress $\bar{\tau}_{12}=\frac{1}{10q_0}\tau_{12}\left(0,0,-h/3\right)$,

Transverse shear stress $\bar{\tau}_{13}=-\frac{1}{10q_0}\tau_{13}\left(0,b/2,0\right)$,

The coordinate thickness $\bar{x}_3 = x_3 / h$, $D=\frac{h^3 E_C}{12\left(1-\nu^2\right)}$

In this section, we validate the proposed composite shear deformation plate theory (CSDPT) using numerical results. We compare it with various standard high-order shear deformation theories (PSDPT, SSDPT, ESDPT), as well as with the first-order FSDPT and the classical plate theory CPT, as referenced in Mindlin (1951), Timoshenko & Woinowsky-Krieger (1959), Reddy (1984), Touratier (1991) and Karama et al. (2003).

Table 5 presents a comparison of dimensionless deviations between the 'present theory' and the 'standard theories,' indicating minor differences across all theories.

Figures 6 and 7 compellingly demonstrate the robust agreement between the present theory and the established standard theories.

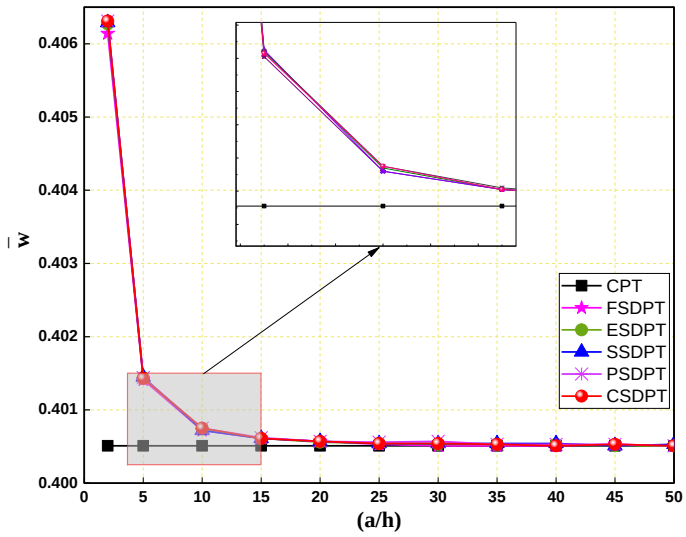

Figure 3 – Dimensionless deflection ($\bar{w}$) across the thickness of a square FGM plate (with n=2) under varied (a/h) ratios, subject to specific conditions (q_0=100, t_i=0)

Table 5 – Comparison of the volume fraction exponent (n) effects on the dimensionless displacements and stresses between the present theory and the established theories.

Deflection	Theory	n = 0	n = 1	n = 2	n = 5	n = 10
$\bar{w}$	CPT	0.83156	1.1896	1.2976	1.3983	1.4878
	FSDT (*)	0.85761	1.2252	1.3382	1.4453	1.5386
	ESDT (*)	0.85743	1.2250	1.3392	1.4482	1.5407
	SSDT (*)	0.85756	1.2251	1.3394	1.4483	1.5410
	TSDT (*)	0.85760	1.2252	1.3394	1.4483	1.5410
	Present	0.85761	1.2252	1.3394	1.4482	1.5410
$\bar{\sigma}_{11}$	CPT	0.50880	0.63901	0.68352	0.75682	0.83819
	FSDT (*)	0.50880	0.63903	0.68355	0.75682	0.83819
	ESDT (*)	0.51180	0.64307	0.68821	0.76210	0.84369
	SSDT (*)	0.51166	0.64286	0.68797	0.76182	0.84343
	TSDT (*)	0.51147	0.64261	0.68769	0.76157	0.84310
	Present	0.51174	0.64298	0.68814	0.76200	0.84357
$\bar{\tau}_{12}$	CPT	0.76599	0.71701	0.69135	0.70066	0.71089
	FSDT (*)	0.76599	0.71701	0.69135	0.70059	0.71093
	ESDT (*)	0.76424	0.71574	0.68985	0.69884	0.70904
	SSDT (*)	0.76437	0.71578	0.68993	0.69893	0.70912
	TSDT (*)	0.76444	0.71582	0.69001	0.69905	0.70920
	Present	0.76430	0.71570	0.68992	0.69890	0.70905
$\bar{\tau}_{13}$	CPT	/	/	/	/	/
	FSDT (*)	-	-	-	-	-
	ESDT (*)	0.34378	0.34378	0.31986	0.29862	0.31141
	SSDT (*)	-	-	-	-	-
	TSDT (*)	0.45704	0.45704	0.44189	0.43013	0.44157
	Present	-	-	-	-	-
		0.44329	0.44329	0.42779	0.41568	0.42766
		-	-	-	-	-
		0.42956	0.42957	0.41372	0.40126	0.41370
		-	-	-	-	-
		0.45200	0.45194	0.43664	0.42471	0.43641

(*) Taken by Bouderba & Berrabah (2022)

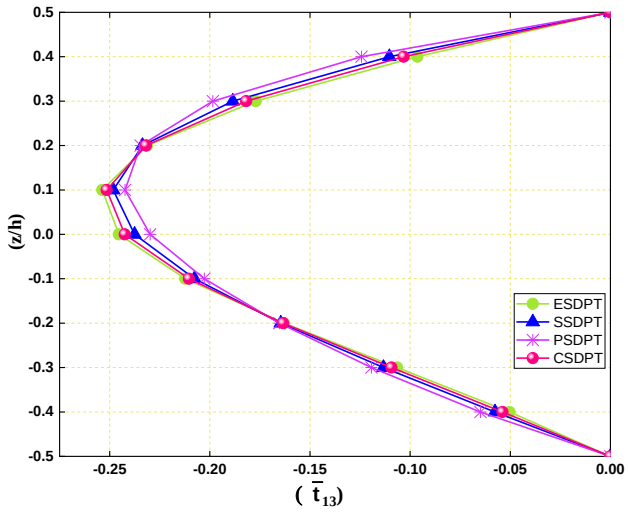

Figure 4 – Variation of ($\bar{\tau}_{13}$) across the thickness of a square FGM plate (with n=2) under varied (a/h) ratios, subject to specific conditions (q_0=100, t_i=0)

The following figures highlight and reveal the influence of the aspect ratios on the stress distribution within functionally graded material plates. A higher a/h (e.g., a/h = 20) results in elevated stress levels, while a lower a/h (e.g., a/h = 2) leads to minimized stress levels, particularly suitable for low-stress-tolerance applications. These findings underscore the pivotal role of aspect ratios in tailoring FGM plate designs to meet diverse stress requirements.

Simultaneously, varying thermal conditions (T_1, T_2, T_3) significantly shapes stress distribution across all aspect ratios, highlighting the pronounced influence of the thermal.

T_3 uniquely impacts the stress gradient through the plate's thickness, highlighting its distinct role in stress distribution.

Material property gradients (n values) play a vital role in shaping stress distribution.

Illustrating the relationship between a/h and n, along with the impact of the thermal field, these factors can be adjusted to meet precise design criteria.

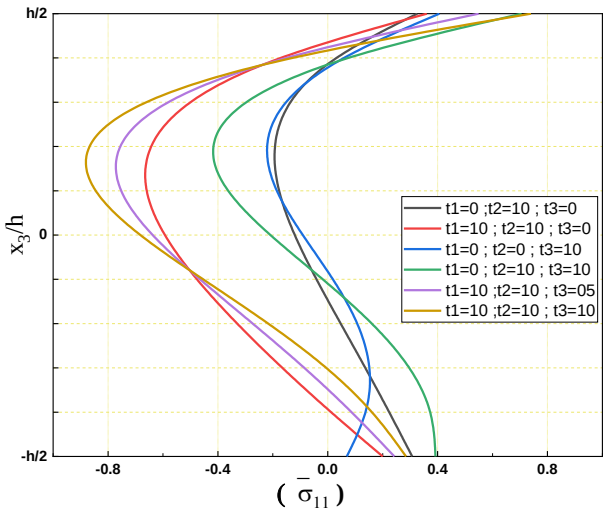

*Figure 5 – Effect of the thermal field on the($\bar{\sigma}_{11}$) through-the-thickness of a rectangular FGM plate with (n = 2, q_0 = 100, b = 2a). a=02*h*

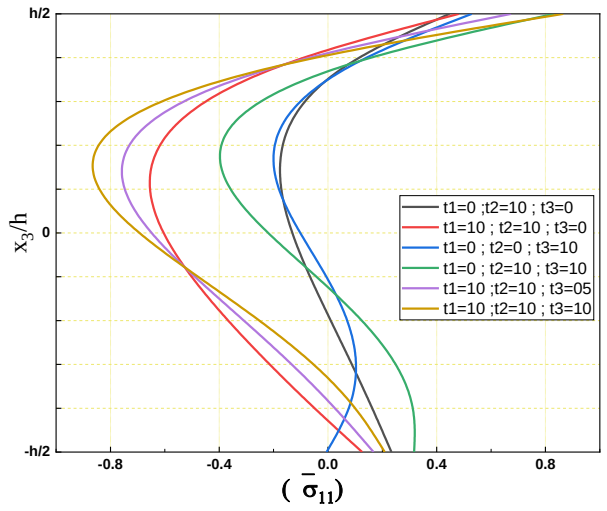

*Figure 6 – Effect of the thermal field on the($\bar{\sigma}_{11}$) through-the-thickness of a rectangular FGM plate with(n = 2, q_0 = 100, b = 2a). a=05*h.*

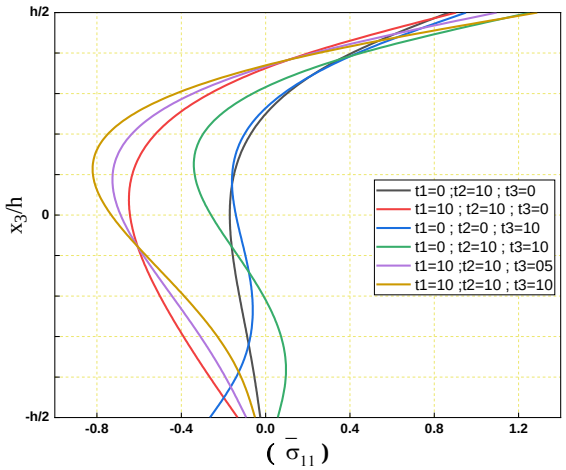

*Figure 7 – Effect of the thermal field on the($\bar{\sigma}_{11}$) through-the-thickness of a rectangular FGM plate with(n = 2, q_0 = 100, b = 2a). a=10*h.*

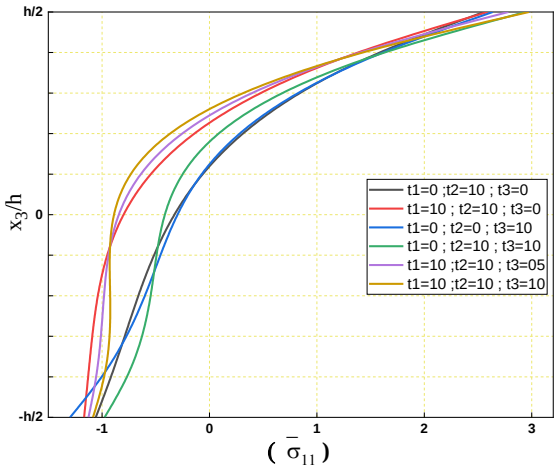

*Figure 8 – Effect of the thermal field on the($\bar{\sigma}_{11}$) through-the-thickness of a rectangular FGM plate with(n = 2, q_0 = 100, b = 2a). a=20*h.*

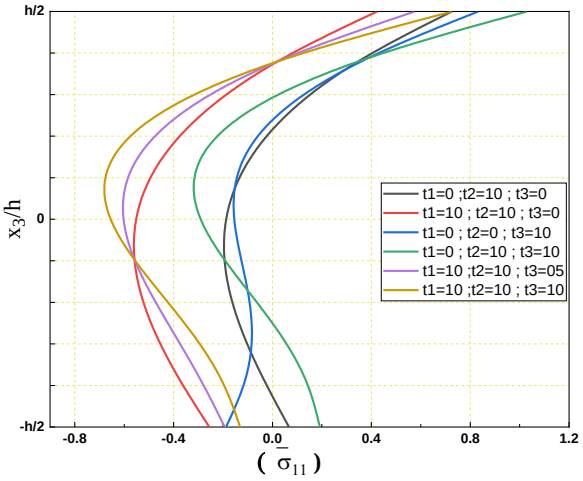

*Figure 9 – Effect of the thermal field on the($\bar{\sigma}_{11}$) through-the-thickness of a rectangular FGM plate with(n = 1, q_0 = 100, b = 2a). a=10*h.*

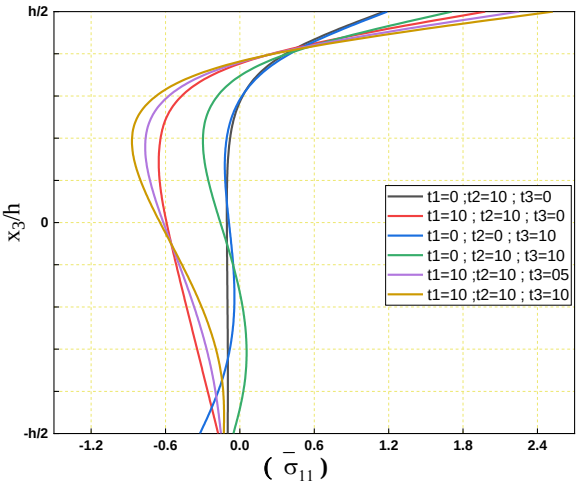

*Figure10 – Effect of the thermal field on the($\bar{\sigma}_{11}$) through-the-thickness of a rectangular FGM plate with(n = 6, q_0 = 100, b = 2a). a=10*h.*

Conclusions

This study thoroughly examined how advanced composite structures respond to various loads - mechanical and thermal - using a new CSDPT theory that eliminates the need for shear correction factors. By comparing the results with the standard established theories, it showed strong consistency being particularly aligned, particularly pertinent when taking into account SSSS boundary conditions. The research explored how changing volume fraction exponents and side-to-thickness ratios impact the displacements and stresses of functionally graded rectangular plates under distributed loading, highlighting the significant influence of material property gradients on their response. It also emphasized how different loads affect stresses within the plates, emphasizing the intricate relationship between these loads and stress distribution. Ultimately, this theory proves to be precise and suitable for analyzing the thermo-mechanical bending response of thick functionally graded plates, contributing valuable insights for practical applications and enhancing our understanding of advanced composite materials.

References

Bao, G. & Wang, L. 1995. Multiple cracking in functionally graded ceramic/metal coatings. *International Journal of Solids and Structures,* 32(19), pp.2853-2871. Available at: https://doi.org/10.1016/0020-7683(94)00267-Z.

Benyamina, A.B., Bouderba, B. & Saoula, A. 2018. Bending response of composite material plates with specific properties, case of a typical FGM “Ceramic/Metal” in thermal environments. *Periodica Polytechnica Civil Engineering*, 62(4), pp.930-938. Available at: https://doi.org/10.3311/PPci.11891.

Berrabah, H.M. & Bouderba, B. 2023. Mechanical buckling analysis of functionally graded plates using an accurate shear deformation theory. *Mechanics of Advanced Materials and Structures*, 30(22), pp.4652-4662. Available at: https://doi.org/10.1080/15376494.2022.2102701.

Boggarapu, V., Gujjala, R., Ojha, S., Acharya, S., Venkateswara babu, P., Chowdary, S. & Gara, D.k. 2021. State of the art in functionally graded materials. *Composite Structures*, 262, pp.113596. Available at: https://doi.org/10.1016/j.compstruct.2021.113596.

Bouazza, M., Tounsi, A., Adda-Bedia, E.A. & Megueni, A. 2011. Thermal buckling of simply supported FGM square plates. *Applied Mechanics and Materials*, 61, pp.25-32. Available at: https://doi.org/10.4028/www.scientific.net/AMM.61.25.

Bouderba, B. & Benyamina, A. B. 2018. Static analysis of composite material plates "Case of a typical ceramic/metal FGM" in thermal environments. *Journal of Materials and Engineering Structures*, 5(1), pp.33-45 [online]. Available at: https://revue.ummto.dz/index.php/JMES/article/view/1606 [Accessed: 01. January 2024].

Bouderba, B. & Berrabah, H.M. 2022. Bending response of porous advanced composite plates under thermomechanical loads. *Mechanics Based Design of Structures and Machines*, 50(9), pp.3262-3282. Available at: https://doi.org/10.1080/15397734.2020.1801464.

Bouderba, B., Houari, M.S.A. & Tounsi, A. 2013. Thermomechanical bending response of FGM thick plates resting on Winkler-Pasternak elastic foundations. *Steel and Composite Structures*, 14(1), pp.85-104. Available at: https://doi.org/10.12989/scs.2013.14.1.085.

Bouderba, B., Houari, M.S.A., Tounsi, A. & Mahmoud, S.R. 2016. Thermal stability of functionally graded sandwich plates using a simple shear deformation theory. *Structural Engineering and Mechanics*, 58(3), pp.397-422. Available at: https://doi.org/10.12989/sem.2016.58.3.397.

Brischetto, S. & Carrera, E. 2010. Advanced mixed theories for bending analysis of functionally graded plates. *Computers & Structures*, 88(23-24), pp.1474-1483. Available at: https://doi.org/10.1016/j.compstruc.2008.04.004.

Brischetto, S., Leetsch, R., Carrera, E., Wallmersperger, T. & Kröplin, B. 2008. Thermo-mechanical bending of functionally graded plates. *Journal of Thermal Stresses*, 31(3), pp.286-308. Available at: https://doi.org/10.1080/01495730701876775.

Daikh, A.A., Bensaid, I. & Zenkour, A.M. 2020. Temperature dependent thermomechanical bending response of functionally graded sandwich plates. *Engineering Research Express*, 2(1), art.number:015006. Available at: https://doi.org/10.1088/2631-8695/ab638c.

Farrokh, M., Afzali, M. & Carrera, E. 2021. Mechanical and thermal buckling loads of rectangular FG plates by using higher-order unified formulation. *Mechanics of Advanced Materials and Structures*, 28(6), pp.608-617. Available at: https://doi.org/10.1080/15376494.2019.1578014.

Farrokh, M., Taheripur, M. & Carrera, E. 2022. Optimum distribution of materials for functionally graded rectangular plates considering thermal buckling. *Composite Structures*, 289, art.number:115401. Available at: https://doi.org/10.1016/j.compstruct.2022.115401.

Karama, M., Afaq, K. & Mistou, S. 2003. Mechanical behaviour of laminated composite beam by the new multi-layered laminated composite structures model with transverse shear stress continuity. *International Journal of solids and structures*, 40(6), pp.1525-1546. Available at: https://doi.org/10.1016/S0020-7683(02)00647-9.

Kieback, B., Neubrand, A. & Riedel, H. 2003. Processing techniques for functionally graded materials. *Materials Science and Engineering: A*, 362(1-2), pp.81-106. Available at: https://doi.org/10.1016/S0921-5093(03)00578-1.

Koizumi, M. 1993. The concept of FGM, functionally graded materials. In: *Ceramic transactions*, 34, pp.3-10. Westerville: American Ceramic Society.

Koizumi, M. 1997. FGM activities in Japan. *Composites part B: Engineering*, 28(1-2), pp.1-4. Available at: https://doi.org/10.1016/S1359-8368(96)00016-9.

Koizumi, M. & Niino M. 1995. Overview of FGM research in Japan. *MRS Bulletin*, 20(1), pp.19-21. Available at: https://doi.org/10.1557/S0883769400048867.

Li, M., Guedes Soares, C. & Yan, R. 2020. A novel shear deformation theory for static analysis of functionally graded plates. *Composite Structures*, 250, art.number:112559. Available at: https://doi.org/10.1016/j.compstruct.2020.112559.

Mindlin, R.D. 1951. Influence of rotatory inertia and shear on flexural motions of isotropic, elastic plates. *Journal of Applied Mechanics,* 18(1), pp.31-38. Available at: https://doi.org/10.1115/1.4010217.

Pindera, M.-J., Aboudi, J. & Arnold, S.M. 1998. Thermomechanical analysis of functionally graded thermal barrier coatings with different microstructural scales. *Journal of the American Ceramic Society*, 81(6), pp.1525-1536. Available at: https://doi.org/10.1111/j.1151-2916.1998.tb02512.x.

Reddy, J.N. 1984. A simple higher-order theory for laminated composite plates. *Journal of Applied Mechanics*, 51(4), pp.745-752. Available at: https://doi.org/10.1115/1.3167719.

Reddy, J.N. 2000. Analysis of functionally graded plates. *International Journal for Numerical Methods in Engineering*, 47(1-3), pp.663-684. Available at: https://doi.org/10.1002/(SICI)1097-0207(20000110/30)47:1/3<663::AID-NME787>3.0.CO;2-8.

Reissner, E. 1945. The effect of transverse shear deformation on the bending of elastic plates. *ASME Journal of Applied Mechanics*, 12(2), pp.A69-A77. Available at: https://doi.org/10.1115/1.4009435.

Shinde, B.M., Sayyad, A.S. & Ghumare, S.M. 2015. A refined shear deformation theory for bending analysis of isotropic and orthotropic plates under various loading conditions. *Journal of Materials and Engineering Structures «JMES»*, 2(1), pp.3-15 [online]. Available at: https://revue.ummto.dz/index.php/JMES/article/view/336 [Accessed: 01 January 2024],

Soldatos, K.P. 1992. A transverse shear deformation theory for homogeneous monoclinic plates. *Acta Mechanica*, 94(3-4), pp.195-220. Available at: https://doi.org/10.1007/BF01176650.

Timoshenko, S. & Woinowsky-Krieger, S. 1959. *Theory of plates and shells*, *Second Edition*. New York: McGraw-Hill. ISBN: 0-07-064779-8.

Touratier, M. 1991. An efficient standard plate theory. *International journal of engineering science*, 29(8), pp.901-916. Available at: https://doi.org/10.1016/0020-7225(91)90165-Y.

Zenkour, A. & Alghamdi, N.A. 2010. Bending analysis of functionally graded sandwich plates under the effect of mechanical and thermal loads. *Mechanics of Advanced Materials and Structures*, 17(6), pp.419-432. Available at: https://doi.org/10.1080/15376494.2010.483323.

Zenkour, A.M. & Hafed, Z.S. 2020. Bending analysis of functionally graded piezoelectric plates via quasi-3D trigonometric theory. *Mechanics of Advanced Materials and Structures*, 27(18), pp.1551-1562. Available at: https://doi.org/10.1080/15376494.2018.1516325.

Examen de flexión de estructuras compuestas de generación avanzada con propiedades específicas expuestas a diferentes cargas

Ahmed Zitouni[a], **autor de correspondencia,** *Bachir* Bouderba[a], *Abdelkader* Dellal[b], *Hamza Madjid* Berrabah[c]

[a] Universidad de Tissemsilt, Departamento de Ciencia y Tecnología, Laboratorio de estructuras y materiales de ingeniería mecánica, Tissemsilt, República Argelina Democrática y Popular

[b] Universidad Tissemsilt, Departamento de ciencia y tecnología, Tissemsilt, República Argelina Democrática y Popular

[c] Universidad de Relizane, Departamento de Ingeniería Civil, Laboratorio de Estructuras y Materiales de Ingeniería Mecánica, Relizane, República Argelina Democrática y Popular

CAMPO: mecánica
TIPO DE ARTÍCULO: artículo científico original

Resumen:

Introducción/objetivo: Este artículo presenta el examen de flexión de estructuras compuestas de generación avanzada con propiedades específicas expuestas a diferentes cargas.

Métodos: Este artículo propone e introduce una nueva teoría generalizada de la deformación cortante de cinco variables para calcular la respuesta estática de placas rectangulares funcionalmente graduadas hechas de cerámica y metal. Notablemente, nuestra teoría elimina la necesidad de un factor de corrección de corte y garantiza condiciones de tensión de corte cero en las superficies superior e inferior. Se introducen investigaciones numéricas para interpretar las influencias de las condiciones de carga y las variaciones de potencia del material clasificado funcionalmente, la proporción de módulo, la proporción de aspecto y la proporción de espesor en el comportamiento de flexión de los FGP. Estos análisis luego se comparan con los resultados disponibles en los textos.

Resultados: Los resultados preliminares incluyen un análisis comparativo con las teorías estándar de deformación por corte de orden superior (PSDPT, ESDPT, SSDPT), así como con las teorías de Mindlin y Kirchhoff (FSDPT y CPT).

Conclusión: Nuestra teoría contribuye junto con las teorías establecidas en el campo, proporcionando información valiosa sobre la respuesta termomecánica estática de placas rectangulares funcionalmente graduadas. Esto abarca la influencia de los valores del exponente de la fracción de volumen en los desplazamientos y tensiones adimensionales, el impacto de las relaciones de aspecto en la deflexión y los efectos del campo térmico en la deflexión y las tensiones. Ejemplos numéricos del examen de flexión de estructuras compuestas de generación avanzada

con propiedades específicas expuestas a diferentes cargas demuestran la precisión de la presente teoría.

Palabras claves: materiales funcionalmente graduados, flexión, teorías de deformación por corte de orden superior, termomecánica.

Исследование на изгиб усовершенствованного поколения композитных конструкций со специфическими свойствами, подверженных различным нагрузкам

Ахмед Зитуни[а], **корреспондент**, *Башир* Будерба[а], *Абделькадер* Деллал[б], *Хамза Маджид* Беррабах[в]

[а] Университет Тиссемсилта, факультет науки и технологий, лаборатория конструкций и материалов машиностроения, г. Тиссемсилт, Алжирская Народная Демократическая Республика

[б] Университет Тиссемсилта, Факультет науки и технологий, г. Тиссемсилт, Алжирская Народная Демократическая Республика

[в] Университет Релизана, Факультет гражданского строительства, лаборатория конструкций и материалов машиностроения, г. Релизан, Алжирская Народная Демократическая Республика

РУБРИКА ГРНТИ: 55.09.43 Композиционные материалы
ВИД СТАТЬИ: оригинальная научная статья

Резюме:

Введение/цель: В данной статье представлено исследование на изгиб композитных конструкций нового поколения со специфическими свойствами, подверженных различным нагрузкам.

Методы: В данной статье представлена новая обобщенная теория деформации сдвига с пятью переменными для расчета статического отклика функционально градуированных прямоугольных пластин, изготовленных из керамики и металла. Данная теория исключает необходимость использования поправочного коэффициента сдвига и обеспечивает отсутствие условий деформации сдвига как на верхней, так и на нижней поверхности пластины. Введено численное испытание при интерпретации влияния условий нагрузки и изменений прочности функционально градуированного материала, а также коэффициентов модуля, аспекта и толщины на поведение функционально градуированных пластин при изгибе. Результаты анализа были сопоставлены с результатами, доступными в литературе.

Результаты: Предварительные результаты включают сравнительный анализ со стандартными теориями сдвиговой

деформации высшего порядка (PSDPT, ESDPT, SSDPT), а также теориями Миндлина и Кирхгофа (FSDPT и CPT).

Выводы: Наряду с ранее подтвержденными теориями в этой области, данная теория вносит вклад, предоставляя ценную информацию о статическом термомеханическом отклике функционально градуированных прямоугольных пластин. Он охватывает влияние значений показателя объемной доли на безразмерные смещения и напряжения, влияние коэффициентов аспекта на дефлексию, а также влияние теплового поля на дефлексию и напряжения. Численные примеры испытаний на изгиб усовершенствованного поколения композитных структур со специфическими свойствами, испытанных различными нагрузками, подтверждают точность представленной теории.

Ключевые слова: функционально-сортированные материалы, изгиб, теории сдвиговой деформации высшего порядка, термомеханический.

Испитивање вршено савијањем напредне генерације композитних структура са специфичним својствима изложених различитим оптерећењима

Ахмед Зитуни[а], **аутор за преписку**, *Башир* Будерба[а], *Абделькадер* Делал[б], *Хамза Маџид* Берабах[в]

[а] Универзитет у Тисемсилту, Одсек за науку и технологију, Лабораторија за машинске материјале и конструкције, Тисемсилт, Народна Демократска Република Алжир

[б] Универзитет у Тисемсилту, Одсек за науку и технологију, Тисемсилт, Народна Демократска Република Алжир

[в] Универзитет у Релизану, Одсек за грађевинарство, Лабораторија за машинске материјале и конструкције, Релизане, Народна Демократска Република Алжир

ОБЛАСТ: механика
КАТЕГОРИЈА (ТИП) ЧЛАНКА: оригинални научни рад

Сажетак:

Увод/циљ: У раду је представљено испитивање савијањем напредне генерације композитних структура са специфичним својствима изложених различитим оптерећењима.

Методе: Предлаже се и уводи нова генерализована теорија смицања са пет варијабли ради израчунавања статичког одговора четвртастих функционално градираних керамичко-металних плоча. Теорија елиминише потребу за коришћењем корективног фактора смицања и обезбеђује одсуство услова за деформацију смицањем и на горњој и на доњој површини плоче. Уводи се

нумеричко испитивање за тумачење утицаја услова оптерећења и варијација снаге функционално градираног материјала, као и коефицијената модула, аспекта и дебљине на понашање функционално градираних плоча при савијању. Резултати ових анализа упоређени су са резултатима доступним у литератури.

Резултати: Прелиминарни резултати обухватају компаративну анализу са стандардним теоријама смицања вишег реда (PSDPT, ESDPT, SSDPT), као и са теоријама Миндлина (FSDPT) и Кирхофа (CPT).

Закључак: Заједно са већ потврђеним теоријама у овој области, представљена теорија пружа допринос увидом у статички термомеханички одговор функционално градираних плоча. Он обухвата утицај вредности експонента запреминског удела на недимензионална померања и напоне, утицај коефицијената аспекта на дефлексију, као и ефекте термалног поља на дефлексију и напоне. Нумерички примери испитивања вршеног савијањем напредне генерације композитних структура са специфичним својствима изложених различитим оптерећењима потврђују тачност представљене теорије.

Кључне речи: функционално градирани материјали, савијање, теорије смицања вишег реда, термомеханички.

Paper received on: 23.11.2023.
Manuscript corrections submitted on: 04.03.2024.
Paper accepted for publishing on: 05.03.2024.